

# Magnetic interactions in $\text{Fe}_{1-x}\text{M}_x\text{Sb}_2\text{O}_4$ , $\text{M} = \text{Mg}, \text{Co}$ , deduced from Mössbauer spectroscopy

Frank J. Berry<sup>1</sup>  · Benjamin P. de Laune<sup>1</sup> · Colin Greaves<sup>1</sup> · Hien-Yoong Hah<sup>2</sup> · Charles E. Johnson<sup>2</sup> · Jacqueline A. Johnson<sup>2</sup> · Saeed Kamali<sup>2</sup> · Jose F. Marco<sup>3</sup> · Michael F. Thomas<sup>4</sup> · Mariana J. Whitaker<sup>1</sup>

© The Author(s) 2018

**Abstract** Magnesium- and cobalt- substituted  $\text{FeSb}_2\text{O}_4$ , of composition  $\text{Fe}_{1-x}\text{Mg}_x\text{Sb}_2\text{O}_4$  ( $x = 0.25, 0.50, 0.75$ ) and  $\text{Fe}_{0.25}\text{Co}_{0.75}\text{Sb}_2\text{O}_4$  have been examined by  $^{57}\text{Fe}$  Mössbauer spectroscopy. The complex spectra recorded from the magnetically ordered materials are interpreted in terms of models in which the dominant magnetic interactions occur along the rutile-related chains of  $\text{FeO}_6$  octahedra in the magnetic structure of  $\text{FeSb}_2\text{O}_4$ . In materials of the type  $\text{Fe}_{1-x}\text{Mg}_x\text{Sb}_2\text{O}_4$ , the diamagnetic  $\text{Mg}^{2+}$  ions have no magnetic moment and behave as non-magnetic blocks which disrupt the magnetic interactions in the chains along the  $c$ -axis forming segments of iron-containing chains separated by  $\text{Mg}^{2+}$  ions. In  $\text{Fe}_{0.25}\text{Co}_{0.75}\text{Sb}_2\text{O}_4$  the spectra are composed of components from different configurations of neighbouring  $\text{Fe}^{2+}$  and  $\text{Co}^{2+}$  ions.

## 1 Introduction

The compound  $\text{FeSb}_2\text{O}_4$  occurs naturally as the mineral schafarzikite and is isostructural with the tetragonal form of  $\text{Pb}_3\text{O}_4$  [1, 2]. Its structure, Fig. 1, consists of rutile-related chains of  $\text{FeO}_6$  octahedra along the  $c$ -axis linked by trigonal pyramidal  $\text{Sb}^{3+}$  cations which, being

---

This article is part of the Topical Collection on *Proceedings of the 4th Mediterranean Conference on the Applications of the Mössbauer Effect (MECAME 2018), Zadar, Croatia, 27–31 May 2018*  
Edited by Mira Ristic and Stjepko Krehula

---

✉ Frank J. Berry  
f.j.berry.1@bham.ac.uk

<sup>1</sup> School of Chemistry, The University of Birmingham, Birmingham B15 2TT, UK

<sup>2</sup> Center for Laser Applications, University of Tennessee Space Institute, Tullahoma, TN 37388, USA

<sup>3</sup> Instituto de Química Física “Rocasolano”, CSIC, Serrano 119, 28006 Madrid, Spain

<sup>4</sup> Department of Physics, University of Liverpool, Liverpool L69 3BX, UK

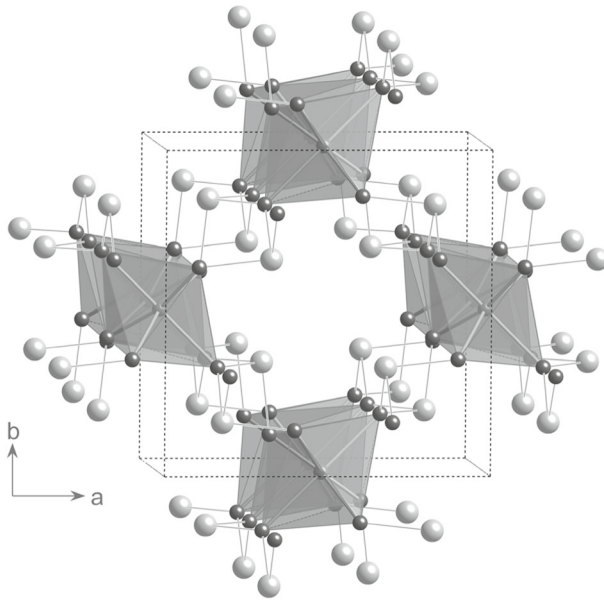


**Fig. 1** The structure of FeSb<sub>2</sub>O<sub>4</sub>: FeO<sub>6</sub> octahedra are shaded with Fe<sup>2+</sup> ions located within the octahedra; O<sup>2-</sup> ions are shown as black spheres and Sb<sup>3+</sup> ions are shown as white spheres

bound to three oxygen anions, possess a lone pair of electrons which can be regarded as a fourth ligand. The Fe-Fe distance within the chains (2.96 Å) is shorter than the nearest Fe-Fe distance within the layers (6.07 Å) and is consistent with some one-dimensional character in FeSb<sub>2</sub>O<sub>4</sub>. The material undergoes an antiferromagnetic transition around 45 K [3, 4]. The <sup>57</sup>Fe Mössbauer spectrum of FeSb<sub>2</sub>O<sub>4</sub> at *ca.* 4.2 K is unusual, being the result of combined magnetic hyperfine and electric quadrupole interactions of comparable strength [5, 6] and, together with data recorded above *T<sub>N</sub>* [7], has been used to determine the order of the *t<sub>2g</sub>* orbital energy levels. The literature also documents some structurally related compounds of composition MSb<sub>2</sub>O<sub>4</sub> (M = Mn<sup>2+</sup>, Co<sup>2+</sup>, Ni<sup>2+</sup>, Cu<sup>2+</sup>, Zn<sup>2+</sup>, Mg<sup>2+</sup>) [8–13].

Although an early attempt to substitute on the Sb site was not successful [14], we subsequently reported the synthesis of materials of composition FeSb<sub>2-x</sub>Pb<sub>x</sub>O<sub>4</sub> [15]. We have also reinvestigated the Mössbauer spectra recorded from FeSb<sub>2</sub>O<sub>4</sub> and found that, in FeSb<sub>2-x</sub>Pb<sub>x</sub>O<sub>4</sub>, the dominant intrachain magnetic exchange gives rise to situations where weakly coupled Fe<sup>2+</sup> ions coexist in a non-magnetic state alongside Fe<sup>3+</sup> ions in a magnetically ordered state [16]. We have also prepared new phases involving substitution on the M site. The magnetic moments deduced from neutron diffraction and magnetic susceptibility measurements in the series of composition Fe<sub>1-x</sub>Co<sub>x</sub>Sb<sub>2</sub>O<sub>4</sub> suggested the existence of some short range correlations within the chains [17] whilst in materials of formulation Fe<sub>1-x</sub>Mg<sub>x</sub>Sb<sub>2</sub>O<sub>4</sub>, the decrease in magnetic ordering temperature with increasing concentrations of magnesium was associated with non-magnetic Mg<sup>2+</sup> ions weakening the magnetic interactions between Fe<sup>2+</sup> ions [18]. An interesting feature of these materials has been the demonstration of their capacity to accommodate additional oxygen within their structures [19].

We report here on the examination of magnetic interactions in the materials Fe<sub>1-x</sub>Mg<sub>x</sub>Sb<sub>2</sub>O<sub>4</sub> and Fe<sub>0.25</sub>Co<sub>0.75</sub>Sb<sub>2</sub>O<sub>4</sub> by <sup>57</sup>Fe Mössbauer spectroscopy and propose

**Table 1**  $^{57}\text{Fe}$  Mössbauer parameters recorded from  $\text{Fe}_{1-x}\text{Mg}_x\text{Sb}_2\text{O}_4$  ( $x = 0.25, 0.50, 0.75$ ) at 16 K

|   | $\delta \pm 0.02$<br>(mm s $^{-1}$ ) | $\Delta$ or $e^2qQ/2 \pm$<br>0.02 (mm s $^{-1}$ ) | $H \pm 0.5$<br>(T) | $\theta$<br>(degree) | $\Psi$<br>(degree) | $\eta$ | Area $\pm$<br>3% |
|---|--------------------------------------|---|--------------------|----------------------|--------------------|--------|------------------|
| $\text{Fe}_{0.25}\text{Mg}_{0.75}\text{Sb}_2\text{O}_4$ | 1.21                                 | 2.89  |                    |                      |                    |        | 100              |
| $\text{Fe}_{0.5}\text{Mg}_{0.5}\text{Sb}_2\text{O}_4$   | 1.26                                 | 2.70  | 12.1               | 38.7                 | 0                  | 0.25   | 22               |
|   | 1.23                                 | 2.94  |                    |                      |                    |        | 78               |
| $\text{Fe}_{0.75}\text{Mg}_{0.25}\text{Sb}_2\text{O}_4$ | 1.24                                 | 2.85  | 17.0               | 63                   | 0                  | 0.25   | 35               |
|   | 1.24                                 | 2.85  | 13.7               | 54                   | 0                  | 0.25   | 38               |
|   | 1.36                                 | 2.85  | 5.0                | 0.1                  | 0                  | 0.25   | 27               |

$\eta$  is the asymmetry parameter (asymmetry of electric field gradient at nucleus);  $\theta$  and  $\Psi$  are the polar and azimuthal angles that specify the direction of the magnetic field, H, with respect to the coordinates of the electric field gradient

models in which the strongest magnetic interactions can be associated with  $\text{Fe}^{2+}$  ions located along the  $c$ -axis in rutile-related  $\text{FeO}_6$  octahedra but which differ according to the magnetic properties of  $\text{Co}^{2+}$  and  $\text{Mg}^{2+}$ .

## 2 Experimental

Materials of composition  $\text{Fe}_{1-x}\text{Mg}_x\text{Sb}_2\text{O}_4$  ( $x = 0.25, 0.5, 0.75$ ) were prepared by heating stoichiometric amounts of  $\text{Fe}_2\text{O}_3$ ,  $\text{MgO}$ ,  $\text{Sb}_2\text{O}_3$  and Sb metal in an alumina crucible within an evacuated sealed silica tube at 650 °C for 60 h.  $\text{Fe}_{0.25}\text{Co}_{0.75}\text{Sb}_2\text{O}_4$  was prepared by heating appropriate amounts of  $\text{Fe}_2\text{O}_3$ ,  $\text{CoO}$ , and  $\text{Sb}_2\text{O}_3$  in an alumina crucible within an evacuated fused silica tube for two six hour periods at 700 °C with intermediate grinding.

The purity of the phases was determined by X-ray powder diffraction at 298 K with a Bruker D8 diffractometer in transmission mode using  $\text{Cu-K}\alpha_1$  radiation.  $^{57}\text{Fe}$  Mössbauer spectra were recorded in constant acceleration mode using a ca. 25 mCi  $^{57}\text{Co}$  source and a helium closed-cycle cryorefrigerator. All the spectra were computer fitted with those recorded at 16 K from  $\text{Fe}_{0.5}\text{Mg}_{0.5}\text{Sb}_2\text{O}_4$ ,  $\text{Fe}_{0.75}\text{Mg}_{0.25}\text{Sb}_2\text{O}_4$  and  $\text{Fe}_{0.25}\text{Co}_{0.75}\text{Sb}_2\text{O}_4$  being fitted using the method of Kundig [20] in which the fitting variables contain not only the energy splitting of the magnetic hyperfine- and electric quadrupole- interactions but also the angle the hyperfine field makes with the principle axis of the electric field gradient. All the chemical isomer shift data are quoted relative to metallic iron at room temperature.

## 3 Results

### 3.1 $\text{Fe}_{1-x}\text{Mg}_x\text{Sb}_2\text{O}_4$ : $x = 0.25, 0.50, 0.75$

The  $^{57}\text{Fe}$  Mössbauer spectral parameters for samples of composition  $\text{Fe}_{1-x}\text{Mg}_x\text{Sb}_2\text{O}_4$  ( $x = 0.25, 0.50$  and  $0.75$ ) at 16 K are contained in Table 1. The spectra shown in Fig. 2 have already been reported [18] but are reproduced here to assist this new discussion in terms of the magnetic interactions in these materials.

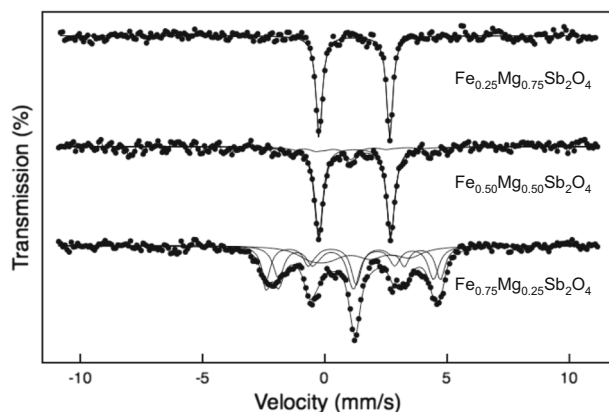


**Fig. 2**  $^{57}\text{Fe}$  Mössbauer spectra recorded from materials of composition  $\text{Fe}_{1-x}\text{Mg}_x\text{Sb}_2\text{O}_4$  at 16 K

At 16 K  $\text{Fe}_{0.25}\text{Mg}_{0.75}\text{Sb}_2\text{O}_4$  shows a quadrupole split absorption characteristic of the paramagnetic state. In contrast the spectrum of  $\text{Fe}_{0.5}\text{Mg}_{0.5}\text{Sb}_2\text{O}_4$  shows a low intensity magnetically split component coexisting with the quadrupole split component (Table 1, Fig. 2). In  $\text{Fe}_{0.75}\text{Mg}_{0.25}\text{Sb}_2\text{O}_4$  the three components required for a best fit to the spectrum (Fig. 2) at 16K all show magnetic splitting with hyperfine field values listed in Table 1.

All features of the spectra are consistent with the magnetisation data reported in reference [18].

### 3.2 $\text{Fe}_{0.25}\text{Co}_{0.75}\text{Sb}_2\text{O}_4$

Mossbauer spectra recorded at 298 K and 76 K showed only quadrupole split absorptions characteristic of paramagnetic  $\text{Fe}^{2+}$  and consistent with the magnetic susceptibility data [17] which indicated a magnetic ordering temperature of *ca* 57 K. The  $^{57}\text{Fe}$  Mössbauer spectra recorded from  $\text{Fe}_{0.25}\text{Co}_{0.75}\text{Sb}_2\text{O}_4$  at 298 K, 76 K and 16 K are shown in Fig. 3 with the  $^{57}\text{Fe}$  Mössbauer parameters collected in Table 2. These spectra are best fitted with components with chemical isomer shifts characteristic of  $\text{Fe}^{2+}$ .

## 4 Discussion

### 4.1 Model of magnetism

The structure of the parent compound,  $\text{FeSb}_2\text{O}_4$ , consists of rutile-like chains of edge-linked  $\text{FeO}_6$  octahedra along the *c*-axis linked by trigonal pyramidal  $\text{Sb}^{3+}$  ions. The short Fe–Fe distance within the chains dominates the magnetic exchange interactions. Where the  $t_{2g}$  orbitals are partly filled, the strongest magnetic coupling involves direct overlap of these orbitals pointing at the linking octahedral edges. When the direct exchange is eliminated, for  $(t_{2g})^6$  configurations, or is small because of poor orbital overlap, superexchange within the chains is significant and involves Fe–O–Fe pathways where the connecting oxygen ions are those of the joining edge between the  $\text{FeO}_6$  octahedra. In  $\text{FeSb}_2\text{O}_4$  magnetic ordering occurs at *ca.* 45 K [3, 4, 15, 18].

In this work we have probed changes in the magnetic behaviour when the cations  $\text{Mg}^{2+}$  and  $\text{Co}^{2+}$  are substituted on to the  $\text{Fe}^{2+}$  sites. The analysis of the results aims to connect

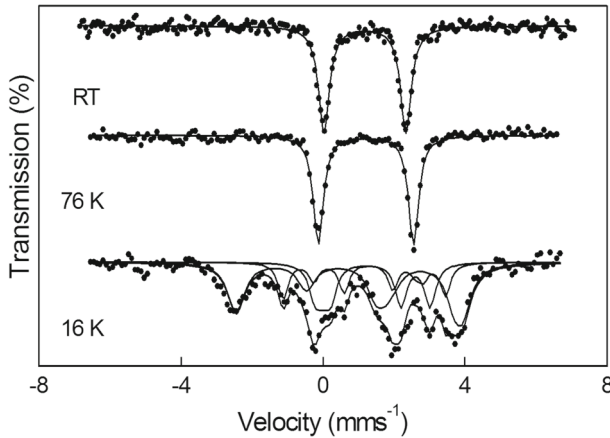


**Fig. 3** <sup>57</sup>Fe Mössbauer spectra recorded from Fe<sub>0.25</sub>Co<sub>0.75</sub>Sb<sub>2</sub>O<sub>4</sub> at 298 K, 76 K and 16 K

features observed in the spectra with the magnetic environments experienced by the iron ions.

The Mg<sup>2+</sup> ion has no magnetic moment and thus behaves as a non-magnetic block to magnetic interactions along the *c*-axis. Thus the effect of Mg<sup>2+</sup> ions is to provide a mixture of iron-containing chains of different lengths along the *c*-axis separated by Mg<sup>2+</sup> ions.

We postulate here that the magnetic behaviour of a given iron-containing segment will depend on the number of iron ions in that segment. At a given temperature below the magnetic ordering temperature (*T<sub>N</sub>*, *ca.* 45 K [3, 4, 15, 18]) isolated iron ions will be more likely to behave paramagnetically while long strings of iron ions will retain magnetic order. This model thus predicts different magnetic behaviour coexisting in the magnetically ordered temperature range because of the different segment lengths. The Mössbauer spectra reported here give insights into this potentially mixed magnetic state.

In the materials of composition Fe<sub>1-x</sub>Mg<sub>x</sub>Sb<sub>2</sub>O<sub>4</sub>, the normalised relative probability that an iron ion is in a segment of *n* iron ions is  $p = n(1-x)^n / \sum n(1-x)^n$  (*n* = 1, ..∞) where (1 - *x*) is the probability that any given cation site on the *c* axis is occupied by an Fe ion. Graphs of *p* versus *n* for the iron concentrations (1 - *x*) = 0.25, 0.50 and 0.75 are shown in Fig. 4a, and we have used these to interpret, in a quasi-quantitative manner, the magnetic behaviour manifested in the Mössbauer spectra.

In Fe<sub>0.25</sub>Co<sub>0.75</sub>Sb<sub>2</sub>O<sub>4</sub> the minority Fe<sup>2+</sup> ions separate segments of Co<sup>2+</sup>. At the end points of this system FeSb<sub>2</sub>O<sub>4</sub> orders magnetically at 45 K in an A type configuration while CoSb<sub>2</sub>O<sub>4</sub> orders at 79 K in a C type configuration [17]. Thus Fe<sup>2+</sup>- Fe<sup>2+</sup> and Fe<sup>2+</sup> - Co<sup>2+</sup> magnetic interactions will shape the Fe<sup>2+</sup> Mossbauer spectrum and we attempt to interpret this via local environments.

#### 4.2 Spectra of Fe<sub>1-x</sub>Mg<sub>x</sub>Sb<sub>2</sub>O<sub>4</sub>: *x* = 0.25, 0.50, 0.75 at 16 K

The spectra from materials in which (1-*x*) = 0.75, 0.50 and 0.25 at 16K are shown in Fig. 2 and the fitting parameters are listed in Table 1.

The overall shape of the magnetic spectrum of Fe<sub>0.75</sub>Mg<sub>0.25</sub>Sb<sub>2</sub>O<sub>4</sub> at 16 K, while similar to that of the parent material FeSb<sub>2</sub>O<sub>4</sub> at ~30 K, now requires three components for a good fit. Comparing the areas of fitted components of a spectrum with areas under the *p*(*n*)

**Table 2**  $^{57}\text{Fe}$  Mössbauer parameters recorded from  $\text{Fe}_{0.25}\text{Co}_{0.75}\text{Sb}_2\text{O}_4$ 

| Temperature (K) | $\delta \pm 0.02$ (mm s $^{-1}$ ) | $\Delta$ or $e^2qQ/2 \pm 0.02$ (mm s $^{-1}$ ) | $H \pm 0.5$ (T) | $\theta$ (degree) | $\Psi$ (degree) | $\eta$ | Area $\pm 3\%$ |
|-----------------|-----------------------------------|--|-----------------|-------------------|-----------------|--------|----------------|
| 298             | 1.18                              | 2.31   | –               |                   |                 |        | 100            |
| 76              | 1.21                              | 2.69   | –               |                   |                 |        | 100            |
| 16              | 1.31                              | 2.61   | 2.6             | 0                 | 0               | 0      | 27             |
|                 | 1.19                              | 2.62   | 16.4            | 90                | 0               | 0      | 50             |
|                 | 1.23                              | 2.87   | 7.2             | 64.5              | 0               | 0      | 23             |

$\eta$  is the asymmetry parameter (asymmetry of electric field gradient at nucleus);  $\theta$  and  $\Psi$  are the polar and azimuthal angles that specify the direction of the magnetic field, H, with respect to the coordinates of the electric field gradient

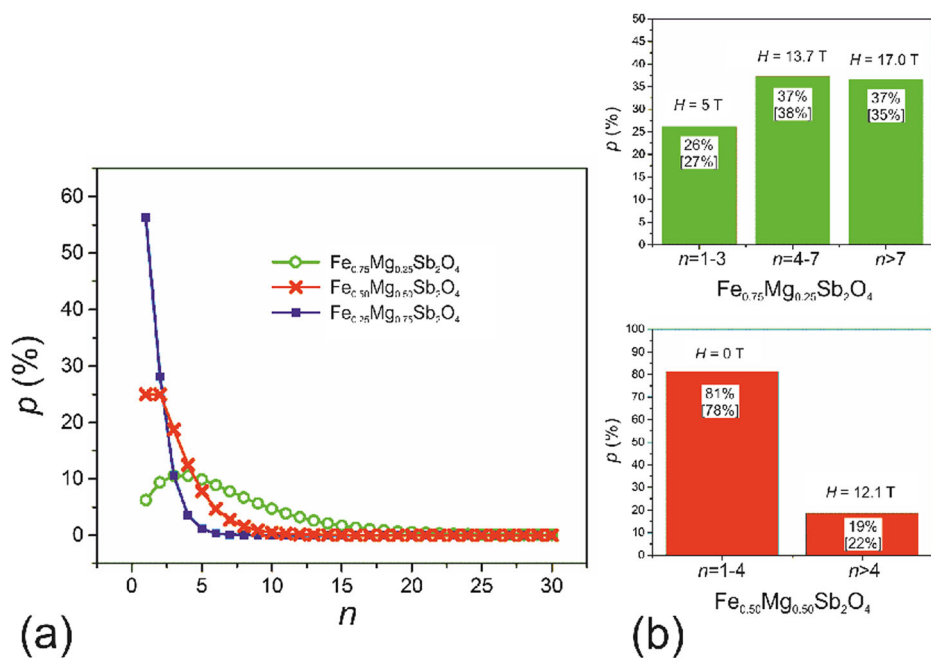


**Fig. 4** **a** Distributions of  $p$  versus  $n$  for values of  $(1-x) = 0.25, 0.50$  and  $0.75$  in  $\text{Fe}_{1-x}\text{Mg}_x\text{Sb}_2\text{O}_4$  ( $M=\text{Mg},\text{Co}$ ); **b** Summary of magnetic states found at 16 K in  $\text{Fe}_{1-x}\text{Mg}_x\text{Sb}_2\text{O}_4$ .  $H$  = magnetic hyperfine field and  $n$  = number of iron ions in segment. The relative proportions compare the distributions in (a) with the experimental data (in square brackets) from Mössbauer spectroscopy, Table 1

versus  $n$  curves of Fig. 4a we are able to establish the segment lengths ( $n$ ) of  $\text{Fe}^{2+}$  ions that give rise to each magnetic component in the spectrum. This is done by associating longer segment lengths with higher magnetic hyperfine fields, justified by assuming that the magnetic anisotropy energy required to reduce the mean spin value  $\langle S \rangle$  by fluctuations is greater the longer length of coupled spins. Values of  $n$ , relating length of segment to each magnetic component in the fitted spectra are given in Fig. 4b where it is seen that for  $\text{Fe}_{0.75}\text{Mg}_{0.25}\text{Sb}_2\text{O}_4$  the components in the spectra with hyperfine field values of 17.0 T,

13.7 T and 5.0 T are associated with segments having  $n > 7$ ,  $7 > n > 4$  and  $n < 4$  respectively.

In  $\text{Fe}_{0.50}\text{Mg}_{0.50}\text{Sb}_2\text{O}_4$  at 16K only segments with  $n > 4$  give a magnetic component.

More data are required to test this model more fully but it supplies a framework to explain the spectra and gives estimates of the lengths of magnetic segments involved.

### 4.3 Spectrum of $\text{Fe}_{0.25}\text{Co}_{0.75}\text{Sb}_2\text{O}_4$ at 16 K

The distributions of  $p$  versus  $n$  for  $\text{Fe}_{0.25}\text{Mg}_{0.75}\text{Sb}_2\text{O}_4$  in Fig. 4a also apply to  $\text{Fe}_{0.25}\text{Co}_{0.75}\text{Sb}_2\text{O}_4$  where the majority magnetic ions are  $\text{Co}^{2+}$  with the  $\text{Fe}^{2+}$  ion segments being very short. In this distribution the probability,  $p$ , of an  $\text{Fe}^{2+}$  ion having values  $n = 1$ , 2 and  $> 2$  are  $p = 56\%$ ,  $28\%$  and  $16\%$  respectively. These values correspond to the  $\text{Fe}^{2+}$  ion having local environments along the  $c$ -axis of two  $\text{Co}^{2+}$  neighbours, one  $\text{Co}^{2+}$  and one  $\text{Fe}^{2+}$  neighbour and two  $\text{Fe}^{2+}$  neighbours respectively. Identifying these  $p$  values with the areas of the fitted components, listed in Table 2, with hyperfine fields of 16.4 T, 7.2 T and 2.6 T gives reasonable agreement suggesting that there is stronger magnetic coupling between  $\text{Fe}^{2+} - \text{Co}^{2+}$  than between  $\text{Fe}^{2+} - \text{Fe}^{2+}$  ions. This simple approach supports the picture that these Mossbauer spectra are largely shaped by the extreme local environment of the  $\text{Fe}^{2+}$  ions.

## 5 Conclusions

The interpretation of the detailed features of the Mössbauer spectra recorded from magnetically ordered materials created by substitution of magnesium or cobalt ions into the parent material  $\text{FeSb}_2\text{O}_4$  are accounted for by a model in which the magnetic structure is quasi one dimensional with the dominant interactions along the  $c$ -axis of the rutile-related chains. Variations of detail arise from local configurations of cations within these rutile-related chains.

**Acknowledgments** We thank the Engineering and Physical Science Research Council for financial support of this research (EPSRC EP/L014114/1) and also acknowledge financial support from Spanish MINECO (Project MAT 2015-64110-C2-1-P). Data associated with the results shown in this paper are accessible from the University of Birmingham Archive: <http://epapers.bham.ac.uk/3097/>.

**Open Access** This article is distributed under the terms of the Creative Commons Attribution 4.0 International License (<http://creativecommons.org/licenses/by/4.0/>), which permits unrestricted use, distribution, and reproduction in any medium, provided you give appropriate credit to the original author(s) and the source, provide a link to the Creative Commons license, and indicate if changes were made.

## References

1. Gavarrí, J.R., Vigouroux, J.P., Calvarin, G., Hewat, A.W.: J. Solid State Chem. **36**, 81–90 (1981)
2. Fischer, R., Pertlik, F.: Tschermarks Mineral. Petrogr. Mitt. **22**, 236–241 (1975)
3. Gonzalo, J.A., Cox, D.E., Shirane, G.: Phys. Rev. **147**, 415–418 (1966)
4. Chater, R., Gavarrí, J.R., Hewat, A.W.: J. Solid State Chem. **60**, 78 (1985)
5. Varret, F., Imbert, P., Gerard, A., Hartmann-Boutron, F.: Solid State Commun. **6**, 889 (1968)
6. Pettit, G., Meder, M.R.: Hyperfine Interact. **5**, 323 (1978)
7. Eibschutz, M., Ganiel, U.: Solid State Commun. **6**, 775 (1968)
8. Tammann, G.: Z. Anorg. Allg. Chem. **149**, 21–34 (1925)

9. Koyama, E., Nakai, I., Nagashima, K.: *Nippon Kagaku Kaishi* **6**, 793–795 (1979)
10. Gavarrri, J.R., Calvarin, G., Chardon, B.: *J. Solid State Chem.* **47**, 132–142 (1983)
11. Witteveen, H.T.: *Solid State Commun.* **9**, 1313–1315 (1971)
12. Ståhl, S.: *Ark. Khem. Min. Geol.* **17 B**, 1–7 (1943)
13. Atanasova, M.T., Strydom, A.M., Schutte, C.J.H., Prinsloo, L.C., Focke, W.W.: *J. Mater. Sci.* **49**, 3497–3510 (2014)
14. Abakumov, A.M., Rozova, M.G., Antipov, E.V., Hadermann, J., Van Tendeloo, G., Lobanov, M., Greenblatt, M., Croft, M., Tsiper, E.V., Llobet, A., Lokshin, K.A., Zhao, Y.: *Chem. Mater.* **17**, 1123–1134 (2005)
15. Whitaker, M.J., Bayliss, R.D., Berry, F.J., Greaves, C.: *J. Mater. Chem.* **21**, 14523–14529 (2011)
16. Bayliss, R.D., Berry, F.J., de Laune, B.P., Greaves, C., Helgason, O., Marco, J.F., Thomas, M.F., Vergara, L., Whitaker, M.J.: *J. Phys.: Condens. Matter* **24**, 276001 (2012)
17. Cumby, J., de Laune, B.P., Greaves, C.: *J. Mater. Chem. C* **4**, 201–208 (2016)
18. de Laune, B.P., Whitaker, M.J., Marco, J.F., Thomas, M.F., Berry, F.J., Lees, M.R., Greaves, C.: *J. Mater. Chem. C* **5**, 4985 (2017)
19. de Laune, B.P., Rees, G.J., Whitaker, M.J., Hah, H.-Y., Johnson, C., Johnson, J.A., Brown, D.E., Tucker, M.G., Hansen, T.C., Berry, F.J., Hanna, J.V., Greaves, C.: *Inorg. Chem.* **56**, 594 (2017)
20. Kundig, W.: *Nucl. Instrum. Methods* **48**, 219 (1967)